

## Impact of High- $k$ $\text{HfO}_2$ Dielectric on the Low-Frequency Noise Behaviors in Amorphous InGaZnO Thin Film Transistors

Jae Chul Park, Sun Il Kim, Chang Jung Kim, Sungchul Kim<sup>1</sup>, Dae Hwan Kim<sup>1</sup>, In-Tak Cho<sup>2</sup>, and Hyuck-In Kwon<sup>3\*</sup>

Semiconductor Laboratory, Samsung Advanced Institute of Technology, Yongin, Gyeonggi 446-712, Korea

<sup>1</sup>School of Electrical Engineering, Kookmin University, Seoul 136-702, Korea

<sup>2</sup>Inter-University Semiconductor Research Center, Seoul National University, Seoul 151-742, Korea

<sup>3</sup>School of Electrical and Electronics Engineering, Chung-Ang University, Seoul 156-756, Korea

Received July 23, 2010; accepted August 20, 2010; published online October 5, 2010

We have investigated the impact of high- $k$   $\text{HfO}_2$  gate dielectric on the low-frequency noise (LFN) behaviors of amorphous indium–gallium–zinc oxide thin-film transistors by comparing the LFNs of devices with  $\text{SiO}_2$  and  $\text{HfO}_2$  dielectrics. Measured LFNs are nearly  $1/f$  type for both devices, but the normalized noise for the  $\text{HfO}_2$  device is around one order of magnitude higher than that for the  $\text{SiO}_2$  device. The bulk mobility fluctuation is considered as the dominant LFN mechanism in both devices, and the increased LFN in the  $\text{HfO}_2$  device is attributed to the enhanced mobility fluctuation by the remote phonon scattering from the  $\text{HfO}_2$ . © 2010 The Japan Society of Applied Physics

DOI: 10.1143/JJAP.49.100205

Since the first report by Nomura *et al.*,<sup>1)</sup> amorphous indium–gallium–zinc oxide (a-IGZO) thin-film transistors (TFTs) have attracted much attention due to their excellent electrical and optical characteristics.<sup>2)</sup> Recently, much effort has been made to reduce the operation voltage of a-IGZO TFTs by incorporating high- $k$  dielectrics for the use of the device in mobile systems.<sup>3–5)</sup> Several groups reported promising results with high- $k$  dielectrics in a-IGZO TFTs.<sup>3,4)</sup> However, high defect densities in high- $k$  dielectrics and high- $k$  dielectric/channel interfaces have been known to cause the adverse effects in device performances.<sup>5)</sup> In this paper, we investigated the impact of high- $k$   $\text{HfO}_2$  dielectric on the low-frequency noise (LFN) behaviors in a-IGZO TFTs. LFN is a powerful tool for the assessment of gate dielectric quality, and it is necessary to reduce the LFN for the implementation of high-performance analog circuits. Although the LFN behaviors of metal–oxide–semiconductor field-effect transistors (MOSFETs)<sup>6)</sup> and amorphous silicon (a-Si) TFTs<sup>7)</sup> have been studied by many authors, very little is known about the LFN behaviors of a-IGZO TFTs yet.<sup>8)</sup> This work is the first report on the LFN behaviors of the a-IGZO TFTs with a representative high- $k$  gate dielectric material,  $\text{HfO}_2$  ( $k \sim 25$ ).

Figure 1(a) shows the schematic cross-section of fabricated a-IGZO TFTs with a staggered bottom gate structure. Devices are fabricated as follows: molybdenum (Mo) as a gate metal was deposited and patterned by a conventional photolithography on a thermally grown  $\text{SiO}_2$ /silicon substrate. Then, 20-nm-thick  $\text{HfO}_2$  was deposited by atomic layer deposition (ALD) method at  $150^\circ\text{C}$  followed by plasma-enhanced chemical vapor deposition (PECVD) deposition of a  $\text{SiO}_2$  (= 100 nm) at  $300^\circ\text{C}$ . The sample with a PECVD deposited  $\text{SiO}_2$  (= 120 nm) was prepared to fabricate a reference device. As an active layer, a-IGZO layer (= 50 nm, a-IGZO target;  $\text{Ga}_2\text{O}_3 : \text{In}_2\text{O}_3 : \text{ZnO} = 2 : 2 : 1$  at.%) was deposited by radio-frequency (RF) magnetron sputtering at room temperature (RT) in a mixed  $\text{Ar}/\text{O}_2$  (100 : 1 at. sccm). For the source/drain, a 200-nm-thick Mo was sputtered at RT and then patterned by dry-etching. After  $\text{N}_2\text{O}$  plasma treatment on the channel surface of the a-IGZO active layer, a  $\text{SiO}_2$  passivation layer was continuously deposited at  $150^\circ\text{C}$  by PECVD without a

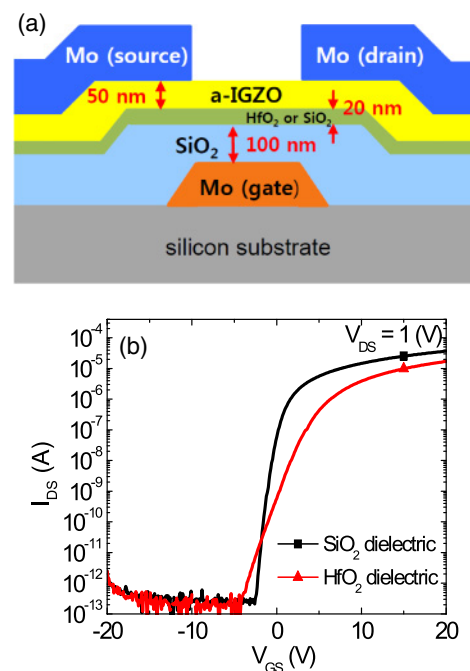


**Fig. 1.** (Color online) (a) Schematic cross-section of the fabricated bottom gate a-IGZO TFTs with  $\text{SiO}_2$  and  $\text{HfO}_2$  dielectrics. (b) Representative transfer curves of the a-IGZO TFTs with  $\text{SiO}_2$  and  $\text{HfO}_2$  dielectrics measured at drain-to-source voltage ( $V_{\text{DS}}$ ) of 1.0 V.

vacuum break. The channel length ( $L$ ), the channel width ( $W$ ), and the length of the overlap region between the gate and source/drain were designed to be 10, 50, and  $10\ \mu\text{m}$ , respectively.

Figure 1(b) shows the representative transfer curves of the a-IGZO TFTs with  $\text{SiO}_2$  and  $\text{HfO}_2$  interfacial dielectric layers. For the a-IGZO TFT with a  $\text{SiO}_2$  interfacial dielectric layer, the subthreshold slope ( $S$ ), field-effect mobility ( $\mu_{\text{FE}}$ ), turn-on voltage ( $V_{\text{ON}}$ ), and threshold voltage ( $V_{\text{TH}}$ ) are 0.36 V/dec,  $16.2\ \text{cm}^2\ \text{V}^{-1}\ \text{s}^{-1}$ ,  $-2.6\ \text{V}$ , and 1.7 V, respectively. The  $\mu_{\text{FE}}$  was determined by the maximum transconductance at a low drain-to-source voltage ( $V_{\text{DS}} = 1.0\ \text{V}$ ).<sup>5)</sup> These electrical parameters are comparable to those of the a-IGZO TFTs in recently published literature works.<sup>2)</sup> On the other hand, the a-IGZO TFT with a  $\text{HfO}_2$  interfacial dielectric layer exhibits the  $S$  of 1.30 V/dec,  $\mu_{\text{FE}}$  of  $9.4\ \text{cm}^2\ \text{V}^{-1}\ \text{s}^{-1}$ ,  $V_{\text{ON}}$  of  $-4.2\ \text{V}$ , and  $V_{\text{TH}}$  of 6.4 V. It can be

\*E-mail address: hyuckin@cau.ac.kr

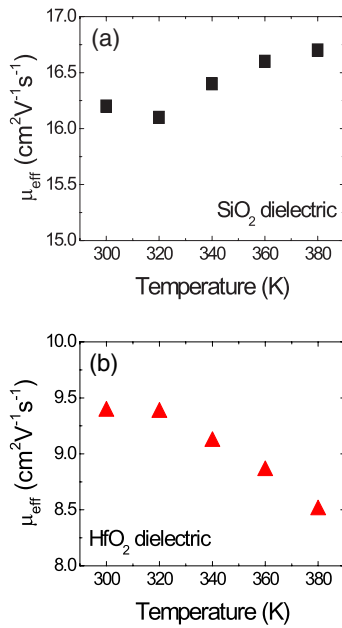


**Fig. 2.** (Color online) Temperature-dependent field-effect mobility ( $\mu_{FE}$ ) of the a-IGZO TFTs with (a) SiO<sub>2</sub> and (b) HfO<sub>2</sub> dielectrics.

seen that the  $S$  value for the HfO<sub>2</sub> device is much larger than that of the SiO<sub>2</sub> device, suggesting that the interfacial trap density of the HfO<sub>2</sub> device is higher than that of the SiO<sub>2</sub> device. Notable degradation of  $\mu_{FE}$  is also observed in the HfO<sub>2</sub> device. Generally, the mobility degradation in high- $k$  transistors is known to be caused from the remote phonon scattering,<sup>9)</sup> Coulomb scattering,<sup>10)</sup> and surface roughness scattering.<sup>11)</sup> In this article, we made use of the classical Mathiessen's rule and the experimental temperature dependence of the scattering terms<sup>12)</sup> to investigate the dominant scattering mechanism causing the mobility degradation in a-IGZO TFTs with HfO<sub>2</sub> gate dielectrics. From Mathiessen's rule

$$\frac{1}{\mu_{eff}} = \frac{1}{\mu_{ph}} + \frac{1}{\mu_{sr}} + \frac{1}{\mu_{cb}} = \beta T^\alpha + \gamma + \frac{\delta}{T}, \quad (1)$$

where  $\mu_{eff}$ ,  $\mu_{ph}$ ,  $\mu_{sr}$ , and  $\mu_{cb}$  represents the total effective mobility and mobilities due to phonon scattering, surface roughness scattering, and Coulomb scattering, respectively.  $\alpha$ ,  $\beta$ ,  $\gamma$ , and  $\delta$  are all positive and temperature-independent constants. Figures 2(a) and 2(b) depict the  $\mu_{FE}$ s for the SiO<sub>2</sub> and HfO<sub>2</sub> devices extracted from the transfer curves measured at various temperatures (300, 320, 340, 360, and 380 K). The data shows that the  $\mu_{FE}$  slightly increases with a temperature in the SiO<sub>2</sub> device, but notably decreases with increasing temperature in the HfO<sub>2</sub> device. Considering that the scattering probability for each transverse electron with phonon is enhanced with increasing temperature, and leads to the degradation in the mobility, the results in Fig. 2 represents that the dominant mechanism of the mobility degradation in the HfO<sub>2</sub> device is the enhanced remote phonon scattering from the HfO<sub>2</sub> dielectric.

Figure 3 shows the normalized noise power spectral densities ( $S_I/I_{DS}^2$ s) of both devices for a gate overdrive voltage ( $V_{GS} - V_{TH}$ ) of 1.0 V, where  $I_{DS}$  and  $V_{GS}$  are the drain-to-source current and the gate-to-source voltage, respectively. The noise measurements were performed in a

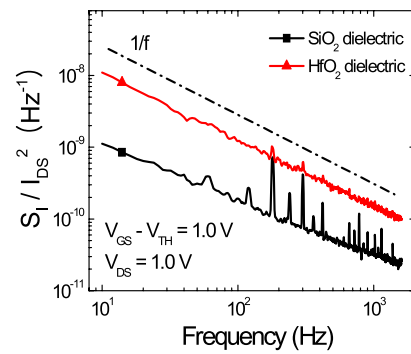


**Fig. 3.** (Color online) Normalized noise power spectral densities ( $S_I/I_{DS}^2$ s) for a-IGZO TFTs with SiO<sub>2</sub> and HfO<sub>2</sub> dielectrics, measured at the same gate overdrive voltage ( $V_{GS} - V_{TH}$ ) of 1.0 V and drain-to source voltage ( $V_{DS}$ ) of 1.0 V.

shield chamber at RT. In both devices, predominantly  $1/f^\gamma$ -like spectra are obtained with a frequency exponent  $\gamma$  of 0.8–0.9. As seen in Fig. 3, the  $S_I/I_{DS}^2$  of the HfO<sub>2</sub> device is around one order of magnitude higher than that of the SiO<sub>2</sub> device.

Generally, there are two major theories to explain the origin of the LFN in transistors. McWhorter originally proposed the carrier number fluctuation theory which considers that the LFN is attributed to the random trapping and detrapping processes of charges in the traps located near the dielectric-channel interface.<sup>13)</sup> Due to the charge fluctuation, the surface potential fluctuates and results in the fluctuation of the channel carrier density. The bulk mobility fluctuation theory based on Hooge's hypothesis considers that the LFN is a result of the fluctuation in the bulk mobility which is induced by fluctuations in phonon popular through phonon scattering.<sup>14,15)</sup> One method of finding the dominant mechanism causing the LFN is to investigate the  $S_I/I_{DS}^2$  dependence on the ( $V_{GS} - V_{TH}$ ) at fixed frequencies.<sup>7)</sup> Figure 4(a) shows that the slope in the log–log plot of  $S_I/I_{DS}^2$  against ( $V_{GS} - V_{TH}$ ) is close to  $-1$  at a fixed frequency of 40 Hz for both devices, which represents that the LFN is mainly due to the bulk mobility fluctuation in both dielectric devices.<sup>7)</sup> The constant slope in Fig. 4(a) also suggests that the source/drain contact noise can be negligible, and the noise mainly comes from the intrinsic channel region in fabricated devices.<sup>16)</sup> Because of the different gate bias dependence of the channel and contact noise, the slope should be  $\sim 2$  when the contact is the dominant noise source.<sup>16)</sup> In Fig. 4(a), the slopes are constant as  $\sim -1$ , which represents that the contact noise is negligible in both devices in all overdrive voltages.

Previous reports have shown that the HfO<sub>2</sub> dielectric increases the LFN in silicon-based MOSFETs, and large efforts have been devoted to find out the mechanism causing this phenomenon. One possible mechanism is the increase of carrier trapping/detrapping due to the high density of traps in the bulk or at the interface of the HfO<sub>2</sub> dielectric. Srinivasan *et al.* investigated the LFN behavior of the n- and p-channel MOSFETs with HfO<sub>2</sub> gate dielectric, and reported that the LFN characteristics behave as being predicted by a carrier number fluctuation mechanism caused by a carrier exchange with traps near the interface.<sup>17)</sup> Another possible mechanism is the increase of the electron–phonon scattering

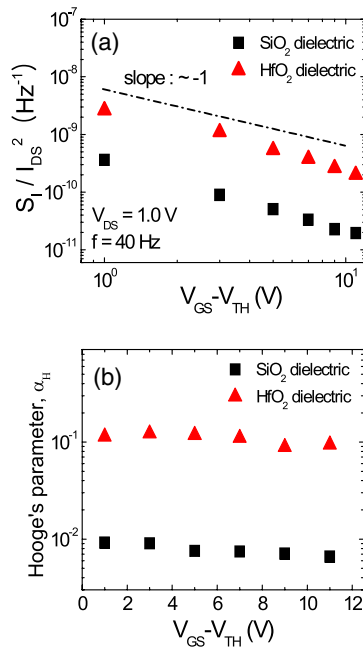


**Fig. 4.** (Color online) (a) Normalized noise power spectral density ( $S_I/I_{DS}^2$ ) versus the gate overdrive voltage ( $V_{GS} - V_{TH}$ ) at a fixed frequency of 40 Hz in a-IGZO TFTs with SiO<sub>2</sub> and HfO<sub>2</sub> dielectrics in the ohmic regime ( $V_{DS} = 1.0$  V). (b) Extracted Hooge's parameters ( $\alpha_H$ ) versus ( $V_{GS} - V_{TH}$ ) for both dielectric devices.

that originates from remote phonon modes in the high-*k*. Haartman *et al.* examined the LFN characteristics of the p-channel MOSFETs with HfO<sub>2</sub> gate dielectric, and reported that the LFN characteristics behave as being expected by a bulk mobility fluctuation mechanism caused by a remote phonon scattering from the HfO<sub>2</sub> dielectric.<sup>18)</sup> Considering that the dominant mechanism of the LFN is the bulk mobility fluctuation in both dielectric devices, the increased LFN of the HfO<sub>2</sub>-dielectric a-IGZO TFT are better explained by the enhanced electron-phonon scattering that originates from the remote phonon modes of the HfO<sub>2</sub>. This is also consistent with our previous conclusion in Fig. 2 that the dominant mechanism of the mobility degradation in the HfO<sub>2</sub> device is the enhanced remote phonon scattering from the HfO<sub>2</sub> dielectric.

When the LFN is primarily due to the bulk mobility fluctuation, the Hooge empirical relation can be applied to analyze the LFNs of the transistors in the ohmic regime:<sup>14)</sup>

$$\frac{S_I}{I^2} = \frac{\alpha_H}{fN}, \quad (2)$$

where  $f$  is the frequency,  $\alpha_H$  is the Hooge's parameter, and  $N$  is the total number of carriers which can be calculated by

$$N = \frac{C_{die}WL}{q} (V_{GS} - V_{TH}), \quad (3)$$

where  $C_{die}$  is the gate dielectric capacitance per unit area and  $q$  is the elementary charge.  $\alpha_H$  is the measure of the LFN magnitude between different devices and can be extracted from eqs. (2) and (3). Figure 4(b) depicts the extracted  $\alpha_H$ s versus ( $V_{GS} - V_{TH}$ ) for both dielectric devices. The extracted  $\alpha_H$ s in the SiO<sub>2</sub> device ( $6.4 \times 10^{-3}$ – $9.1 \times 10^{-3}$ )

are comparable with that of the a-Si TFTs,<sup>7)</sup> and are around one order of lower than that of the polycrystalline silicon TFTs with a same gate dielectric.<sup>19)</sup> The  $\alpha_H$ s in the HfO<sub>2</sub> device ( $8.7 \times 10^{-2}$ – $1.2 \times 10^{-1}$ ) exhibit around one order of higher values than that of the SiO<sub>2</sub> device.

In summary, we have investigated the effect of high-*k* HfO<sub>2</sub> gate dielectric on the electrical characteristics and LFN behaviors of a-IGZO TFTs. Compared to the SiO<sub>2</sub> reference device, substantial degradation of  $S$  and  $\mu_{FE}$  is observed in the HfO<sub>2</sub> device, which is attributed to the higher interface trap density and enhanced remote phonon scattering from the HfO<sub>2</sub> dielectric, respectively. Measured LFNs fit well to a  $1/f^\gamma$  power law with  $\gamma = 0.8$ – $0.9$  in devices with both dielectrics, but  $S_I/I_{DS}^2$  in the HfO<sub>2</sub> device is around one order of magnitude higher than that of the SiO<sub>2</sub> reference device. The ( $V_{GS} - V_{TH}$ ) dependence of  $S_I/I_{DS}^2$  shows that the LFN is mainly attributed to the bulk mobility fluctuation in the intrinsic channel region for both dielectric devices. The main mechanism causing the increase of LFN in the HfO<sub>2</sub> device is ascribed to the enhanced mobility fluctuation noise stemming from remote phonon modes in the high-*k* HfO<sub>2</sub>.

**Acknowledgements** This research was supported by Basic Science Research Program through the National Research Foundation of Korea (NRF) funded by the Ministry of Education, Science and Technology (No. 2009-0068799) and by Mid-career Researcher Program through NRF grant funded by the MEST (No. 2009-0080344).

- 1) K. Nomura, H. Ohta, A. Takagi, T. Kamiya, M. Hirano, and H. Hosono: *Nature* **432** (2004) 488.
- 2) K. Takechi, M. Nakata, T. Eguchi, H. Yamaguchi, and S. Kaneko: *Jpn. J. Appl. Phys.* **48** (2009) 011301.
- 3) Y.-J. Cho, J.-H. Shin, S. M. Bobade, Y.-B. Kim, and D.-K. Choi: *Thin Solid Films* **517** (2009) 4115.
- 4) J. S. Lee, S. Chang, S.-M. Koo, and S. Y. Lee: *IEEE Electron Device Lett.* **31** (2010) 225.
- 5) J.-S. Park, J. K. Jeong, Y.-G. Mo, and S. Kim: *Appl. Phys. Lett.* **94** (2009) 042105.
- 6) M. Marin, Y. A. Allogo, M. de Murcia, P. Linares, and J. C. Vildeuil: *Microelectron. Reliab.* **44** (2004) 1077.
- 7) J. Rhayem, M. Valenza, D. Rigaud, N. Szydlo, and H. Lebrun: *J. Appl. Phys.* **83** (1998) 3660.
- 8) J.-M. Lee, W.-S. Cheong, C.-S. Hwang, I.-T. Cho, H.-I. Kwon, and J.-H. Lee: *IEEE Electron Device Lett.* **30** (2009) 505.
- 9) M. V. Fischetti, D. A. Neumayer, and E. A. Cartier: *J. Appl. Phys.* **90** (2001) 4587.
- 10) L.-A. Raganarsson, L. Pantisano, V. Kaushik, S.-I. Saito, Y. Shimamoto, S. De Gendt, and H. Heyns: *IEDM Tech. Dig.*, 2003, p. 87.
- 11) S. Saito, D. Hisamoto, S. Kimura, and M. Hiratani: *IEDM Tech. Dig.*, 2003, p. 797.
- 12) S. Takagi, A. Toriumi, M. Iwase, and H. Tango: *IEEE Trans. Electron Devices* **41** (1994) 2357.
- 13) A. L. Mc Whorter: in *Semiconductor Surface Physics*, ed. R. H. Kingston (University of Pennsylvania Press, Philadelphia, PA, 1957) p. 207.
- 14) F. N. Hooge: *Phys. Lett. A* **29** (1969) 139.
- 15) R. P. Jindal and A. van der Ziel: *J. Appl. Phys.* **52** (1981) 2884.
- 16) J. M. Peransin, P. Vignaud, D. Rigaud, and L. K. J. Vandamme: *IEEE Trans. Electron Devices* **37** (1990) 2250.
- 17) P. Srinivasan, E. Simoen, L. Pantisano, C. Claeys, and D. Misra: *J. Electrochem. Soc.* **153** (2006) G324.
- 18) M. von Haartman, B. G. Malm, and M. Östling: *IEEE Trans. Electron Devices* **53** (2006) 836.
- 19) A. Mercha, J. Rhayem, L. Pichon, M. Valenza, J. M. Routoure, R. Carin, O. Bonnaud, and D. Rigaud: *Microelectron. Reliab.* **40** (2000) 1891.